NOVEL HIGH STEP-UP DC-DC CONVERTER WITH COUPLED INDUCTOR AND SWITCHED CAPACITOR TECHNIQUES

Mrs.S.REHANA BEGUM, PG Scholar,
Master of Engineering in Power electronics and drives,
C.Abdul Hakeem College of Engineering & Technology,
Melvisharam, Vellore Dt, Tamilnadu

Mr. C.BOOPALAN M.Tech.,
Professor and Head
C.Abdul Hakeem College of Engineering &
Technology, Melvisharam, Vellore Dt, Tamilnadu

ABSTRACT:

This project is presented based on a novel isolated high step-up converter for sustainable energy applications. The suggested structure consists of a coupled inductor and adjustable voltage multiplier module which achieves a high step up gain without utilizing either a large duty ratio or a high turns ratio. During switch off period additional capacitors are charged using the energy stored in the coupled inductor which increases the voltage transfer gain. The energy stored in the leakage inductance recycled using the passive clamp circuit. Hence the stress on the main power switches are reduced with the proposed topology. The added advantage of this project satisfies the electrical isolation and safety regulation. The operating principle, steady state and conduction loss analysis of voltage gain are discussed in detail. Finally a prototype circuit with 40V input voltage 380V output and 500w max output power is implemented in the laboratory to verify performance of the proposed converter.

Keywords:

High step-up, isolated converter voltage-multiplier module, dc-dc converter, coupled inductor, switched capacitor.

I.INTRODUCTION

Renewable energy systems are more widely used as there is a demand for the clean and sustainable energy sources has increased with the growing population and Industrial development. The fuel cells photovoltaic array source are low-voltage source needing step-up dc-dc converter to boost low voltage to high voltage for inverter to feed ac utility although the pv solar cells can be connected in series to get high voltage for grid connected, By using high step-up converter module it can work independently to generate power as micro grid and avoid the effect. In practice the voltage gain is limited by the effect of power switch, rectifier diode and equivalent series resistance(ESR) of inductor and capacitor. Also the extreme high duty-ratio operation may result in serious reverse recovery problem low efficiency and the EMI problem.

The block diagram of a typically sustainable energy system is shown in fig.1. The rated voltage of renewable -energy sources like Pv and fuel cells are at low levels, so that the intermediate converter with a sufficiently high step-up conversion and high efficiency is obtained in this system.

BLOCK DIAGRAM
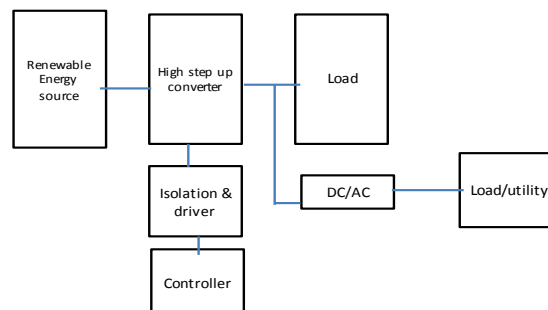
The performance of the step-up converter can be improved by increasing step-up gain without extreme duty cycle and high turns ratio, for increasing efficiency and coupling. the leakage energy must be recycled for improving efficiency and alleviating large voltage spikes on the power switches.

Low voltage stresses on semiconductor devices for adoption of low voltage rated semiconductor devices are required to improve the efficiency.

For the electrical-isolation requirements set forth by industry and market, the development of high step-up converters with electrical isolation is also important and necessary. Unfortunately, many isolated step-up converters without continuous and smooth input current levels result in conducted electromagnetic-interference (EMI) problems [24]–[26]. Thus, a bulky input filter must be designed in order to meet safety regulations. Moreover, such isolated step-up converters need more complex pulse width modulation (PWM) control, which increases cost and decreases reliability.

The proposed high step-up converter with voltage-multiplier modules for sustainable energy applications, which simultaneously satisfies the requirements for electrical-isolation and safety regulations, is shown in Fig. 2.

The advantages of the proposed converter are as follows.

1) Voltage-multiplier modules make the voltage gain higher and voltage stresses lower.
2) The proposed converter possesses continuous and smooth input current, which decreases the conduction losses, lengthens the life time of the input source, and constrains conducted EMI problems.
3) Due to the passive lossless clamped performance, the leakage energy is recycled. Hence, the potential for a large voltage spike across the main switch is alleviated and the efficiency is improved.
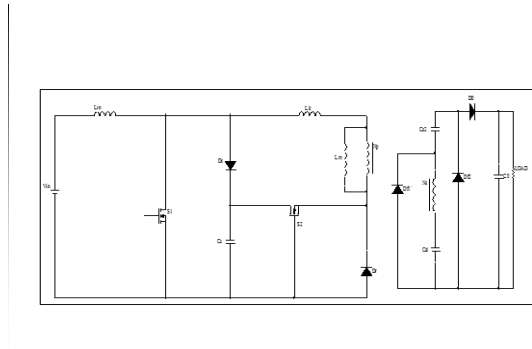

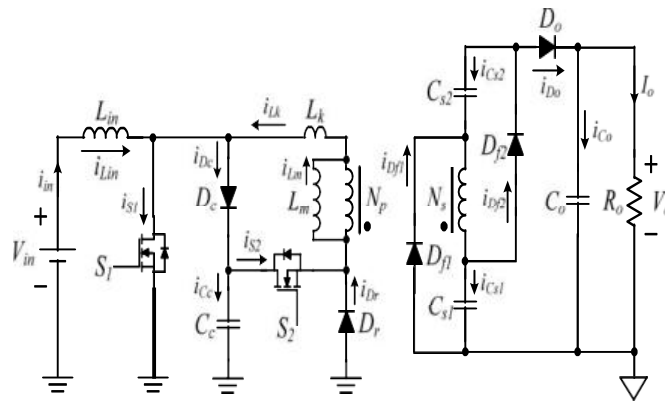Fig. 2 proposed isolated high step-up converter circuit

Fig. 2 proposed isolated high step-up converter Equivalent circuit.

Voltage stresses on the semiconductor devices are substantially lowered. Thus, both low-voltage-rated power switches with low $R_{DS(ON)}$ and low-voltage-rated Schottky diodes without reverse-recovery time can be employed. The sustainable energy source and load possess electrical-isolation characteristic, and the safety regulations is also satisfied.

II. OPERATING PRINCIPLE OF PROPOSED CONVERTER

The equivalent circuit of the proposed isolated converter is shown in Fig. 3, where L_{in} is the input inductor, L_m is the magnetizing inductor, L_k is the leakage inductor, S_1 and S_2 are the power switches, C_c is the clamp capacitor, C_{s1} and C_{s2} are the switched capacitors, and C_o is the output capacitor. D_c is the clamp diode and D_r is the regenerative diode; D_{f1} and D_{f2} represent the diodes of fly back-forward, and D_o represents the output diode. The turns ratio N_s/N_p is defined as n.

In the circuit analysis, the duty cycles of switches during steady operation are the same, and are lower than 0.5. The steady-state waveform under continuous-conduction mode (CCM) operation is depicted in Fig. 4, and the corresponding modes are shown in Fig. 5.

Mode I ($t_0 \nleqslant t < t_1$): At $t = t_0$, both power switches S_1 and S_2 start to turn ON, and the output diode D_O remains in the forward-biased state, as shown in Fig. 5(a). The currents through input inductor L_{in} and leakage inductor L_k increase linearly, and the magnetizing inductor L_m still releases energy to the secondary side of

the coupled inductor due to leakage inductor L_k. In addition, the energy stored in L_m is delivered to output resistor R_o via output diode D_o.
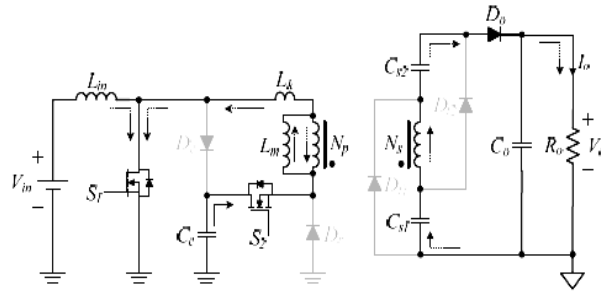
Mode II ($t_1 \leq t < t_2$): At $t = t_1$, all semiconductor devices remain in the previous state except for the diodes in the secondary side of the coupled inductor, as shown in Fig. 5(b). As the current through output diode D_o decreases to zero, the coupled inductor operates in forward mode, which transfers energy to the switched capacitors C_{s1} and C_{s2} via diodes D_{f1} and D_{f2}, respectively. The currents through input inductor L_{in}, magnetizing inductor L_m, and leakage inductor L_k increase linearly.


(b)
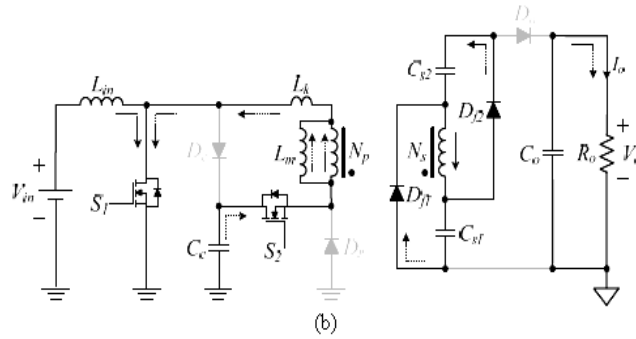
Mode III ($t_2 \leq t < t_3$): At $t = t_2$, both power switches S_1 and S_2 start to turn OFF, and the diodes D_c and D_r are in the forward-biased state, as shown in Fig. 5(c). The input inductor L_{in} and leakage inductor L_k release energy to clamp capacitor C_c via clamp diode D_c; also, the energy stored in the leakage inductor L_k is recycled through the regenerative diode D_r. Thus, the current through leakage inductor L_k speedily and linearly decreases. The magnetizing inductor L_m still absorbs energy from the leakage inductor L_k.


(c)
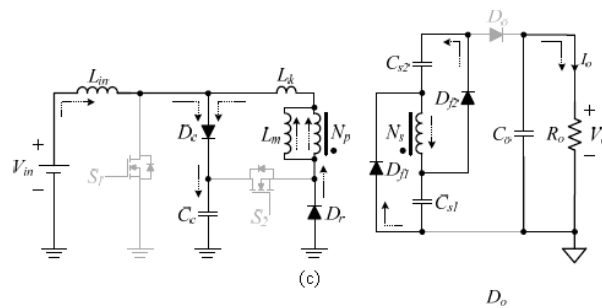
Mode IV ($t_3 \leq t < t_4$): At $t = t_3$, all semiconductor devices remain in the previous state except for the diodes in the secondary side of the coupled inductor, as shown in

Fig.(d) As the currents through diodes D_{f1} and D_{f2} decrease to zero, the coupled inductor operates in fly back mode, and the magnetizing inductor L_m along with switched capacitors C_{s1} and C_{s2} supplies energy to the output resistor R_o via diode D_o.
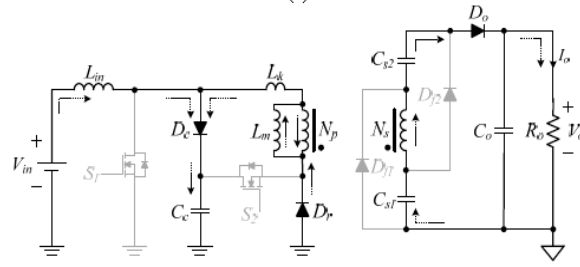
Mode V (t4 ≤ t < t5): At $t = t4$, because the leakage energy is completely recycled, the diode D_r starts to turn OFF naturally, and the other semiconductor devices remain in the previous state, as shown in Fig. 5(e). The input inductor L_{in} and magnetizing inductor L_m still provide energy to the capacitor C_C and the output resistor R_O, respectively, due to CCM operation. At $t = t5$, power switches $S1$ and $S2$ turn on again and the mode I begins again for the next switching cycle.

(e)
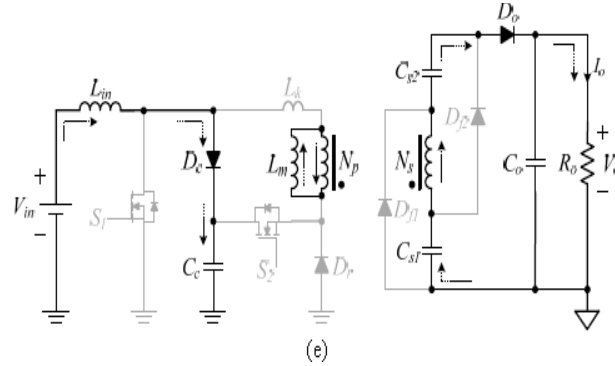
III. STEADY -STATE ANALYSIS OF PROPOSED CONVERTER

The transient characteristics of the circuitry are disregarded and small-ripple approximation is used for calculation: thus all currents that pass through components are approximated by the dc components. some formulated assignments are as below
 1 all of the components in the proposed isolated converter possess ideal characteristics.
2. The coupling coefficient of coupled inductor is unity; therefore there is no need for a leakage inductor.
3. Voltages on the capacitors and current through the magnetizing inductor are considered to be constant due to infinitely large capacitances and inductances.

A. Step-up Gain
The voltages on clamp capacitor Cc can be regarded as an output voltage of the boost converter; thus voltage VCc can be derived from

VCc= 1/ 1-D Vin

When both switches are in the ON state, the voltage on the switched capacitors Cs1 and Cs2 can be obtained as

$VCs1 = VCs2 = n /1−D V_{in}$. (2)

Thus, the output voltage Vo can be derived from

$Vo=VCs1+VCs2+(nD/(1−D)^2)V_{in}=(n(2−D)/(1−D)^2)V_{in}$ (3)

The voltage gain of the proposed converter, illustrated in Fig. , is obtained as $Vo/Vin = n(2−D)/(1− D)^2$ (4)

Equation (4) confirms that the proposed isolated converter has a high step-up voltage gain without an extreme duty cycle or high turns ratio. When the duty cycle is merely 0.5, the voltage gain reaches 6 at a turns ratio n of 1; the voltage gain reaches 30 at a turns ratio n of 5.

B. Voltage Stresses

The voltage stresses on diodes Dc and Dr are equal to VCc, and the voltage stresses on diodes Df1, Df2 and Do are equal to VCo minus VCs1, also equal to VCo minus VCs2. These voltage stresses are given by

$V_{DS1} = 1/1-D \ V_{in} = 1-D/n(2-D)V_o$ (5)

$V_{DS2} = D/(1-D)2V_{in} = D/n(2-D)V_o$ (6)

The voltage stresses on diodes Dc and Dr are equal to V_{Cc} and the voltage stresses on diodes Df1,Df2and Do are equal to VCo minus VCs1 also equal to VCo minus VCs2. These voltage stresses are given by

$V_{Dc} = V_{Dr} = V_{Cc} = (1/1-D)V_{in} = 1-D/n(2-D)V_o$ (7)

$V_{Df1} = V_{Df2} = V_{Do} = V_{Co} - V_{Cs1}$
$= n/(1-D)2V_{in} = 1/(2-D)V_o$ (8)

The relationship between the voltage stresses and the output voltage Vo and turns ratio n under a duty cycle of 0.5 is as shown in the fig. , when the duty cycle is 0.5 the voltage stresses on the semiconductor components located on the primary side of the coupled inductor are the same and are equal to one third of output voltage Vo, even at a turns ratio of n of 1. The voltage stresses on the diode placed on the secondary side of the coupled inductor are the same and although the voltage stresses are larger, the voltage stresses are still lower than the output voltage Vo.

C. Analysis of Conduction Losses

Some conduction losses are caused by resistances of semiconductor components and coupled inductors. Thus, in this section, all the components are not continuously assumed to be ideal, except for all the capacitors. In addition, reverse recovery problems of diodes, leakage inductors, parasitic capacitors, core losses, switching losses, and equivalent series resistance and equivalent series inductance of capacitors are

not discussed in this section. The conduction-loss effect upon voltage gain and efficiency can also be calculated using small ripple approximation, voltage-second balance, and capacitor charge balance. The equivalent circuit, including conduction losses of coupled inductors and semiconductor components, is shown in Fig. 7, in which rLin, rLp, and rLs are, respectively, the copper resistances of the input inductor and the coupled inductor; rDS1 and rDS2 denotes the RDS(ON) of power switches; VDc, VDr, VDf1, VDf2, and VDo represent the forward biases of the Diodes, and rDc, rDr, rDf1, rDf2, and rDo are the resistances of the diodes.

The voltage gain and efficiency with regard to conduction losses are, respectively, given by Vo/ Vin
=
n(2−D)/ (1−D)2 − 1 /Vin · [n(2−D)/ (1−D) ·   VDc+(VDf1 +VDf2 +VDo)

―――――――――――――――――――――――――――――

1+[n(2−D)]2[rLin+X·rDs1+Y ·(rLp+rDS2)] (1−D)4·Ro +(4−3D)·rLs+ RD D(1−D)·Ro (9)
and
η =
1−(1−D)·VDc Vin + (1−D)2 n(2−D) · VDf1+VDf2+VDo Vin ―――――――――――

――――――――――――――――――――――――――――

1+[n(2−D)]2[rLin+X·rDs1+Y ·(rLp+rDS2)] (1−D)4·Ro +(4−3D)·rLs+ RD D(1−D)·Ro (10)

where

X = (1+D)2/D

Y = n2D+(n+D)(1-D)/nD
RD = nD(2−D)2/ (1−D)2 · rDc + D · rDo
        +(1− D)(rDf1 +rDf2)
rLs = n · rLp.

Referring to (10), it can be inferred that the efficiency will be higher if the input voltage is considerably higher than the summation of the forward bias of all diodes, or if the resistance of the load is substantially larger than the combined resistances of input inductor, coupled inductor, and semiconductor components. The calculated voltage gain and calculated efficiency versus duty cycle with different copper resistances of input inductor are shown in Fig. 8, and the other parameters are set as follows:

1) input voltage Vin: 40 V; load Ro: 320;
2) RDS(ON) of power switches rDS1 and rDS2: 10 m; resistances of all diodes rDc, rDf1,rDf2, andrDo:5m;
3) forward biases of all diodes VDc, VDf1, VDf2, and VDo: 0.7V;
4) turns ratio n: 2, and hence the copper resistance in secondary winding rLs is equal to double rLp. The copper resistance in the primary winding rLp and secondary winding rLs are, respectively, equal to 20 and 40 m.
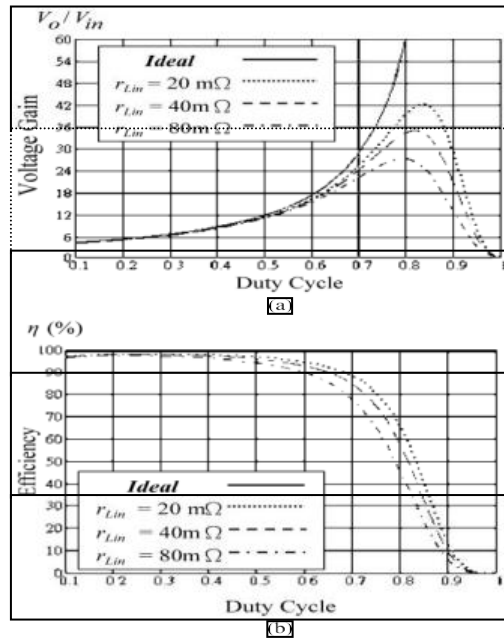

D. Different Applications for Renewable Energy and Low Voltage sources

Some renewable energy sources with low level of voltage, such as a solar cell or a fuel cell stack, require a high step-up conversion for supplying power with loads for high-voltage applications. A high step-up converter not only possesses electric isolation but also is capable to lengthen the lifetime of sources such as battery sets and fuel cell stacks. Thus, the current-fed characteristic for lengthening the lifetime of sources without a large LC filter is also a main design consideration, which makes the power sources or battery sets able to smoothly discharge. For a solar cell system, maximum power point tracking (MPPT) is an important consideration, and MPPT is suitably implemented by a current-fed structure and adjusting the duty cycle within a range. Thus, the proposed converter is also suitable to operate in a solar cell system. Additionally, a tradeoff should be made for practical output power to load between efficiency of the converter and MPPT, because the larger duty cycle causes efficiency to decrease even if the copper resistances decreased by lower turns ratio n.
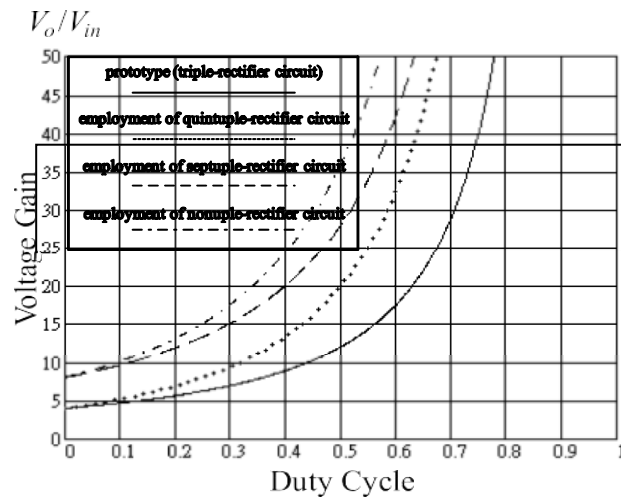
IV FURTHER EXTENSION OF VOLTAGE MULTIPLIER MODULES

For increasing the voltage gain and reducing the voltage

stresses of the proposed isolated converter, the voltage- multiplier modules in the secondary side can be extended by symmetrically multiplicative design. The symmetrically multiplicative design satisfies requirements for low output ripple; examples of these (quintuple-rectifier circuit, septuple- rectifier circuit, and nonuple-rectifier

$$V_{Co} = \frac{n(4-D)}{(1-D)^2} V_{in}$$
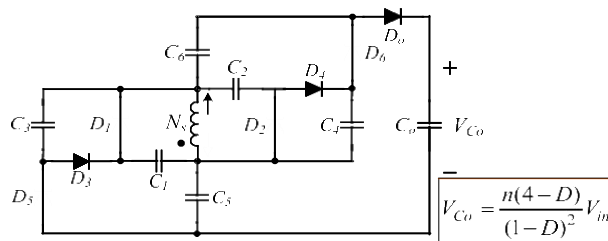
Circuit, and so on) are shown in Fig. 9, where N_s represents the secondary side of the coupled inductor, and V_{Co} indicates the supplied voltage of output capacitors in the secondary side


The principal-characteristic comparison of voltage gains and voltage stresses for the proposed isolated converter among uses of symmetrically multiplicative designs is illustrated in Fig. 10, where the different voltage gains are depicted under the turns-ratio n set as 2, and the different voltage stresses are depicted under the duty-cycle set as 0.5. The principal-characteristics comparison demonstrates that the extension of voltage-multiplier modules by symmetrically multiplicative design effectively causes the voltage gain to increase and the voltage stresses to decrease. However, although the voltage stresses can be reduced, the cost and quantity of capacitors and diodes are increased. Thus, a tradeoff exists between benefits and incidental price , so each symmetrically multiplicative design can be selected based on the given requirement of each application.

$$V_{Co} = \frac{n(4+D)}{(1-D)^2} V_{in}$$

(d)

Turns ratio n
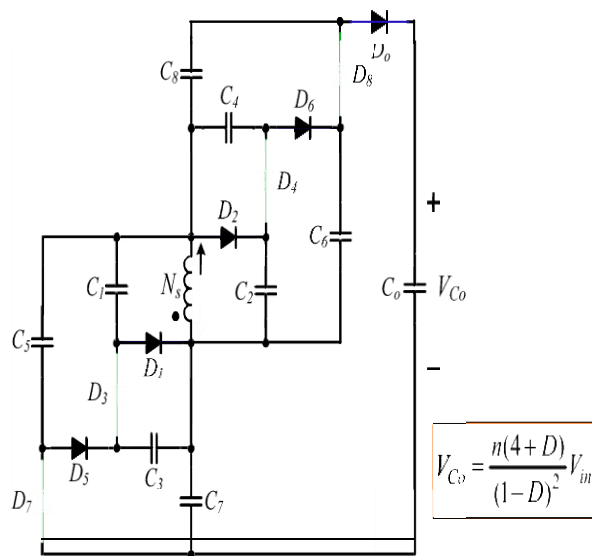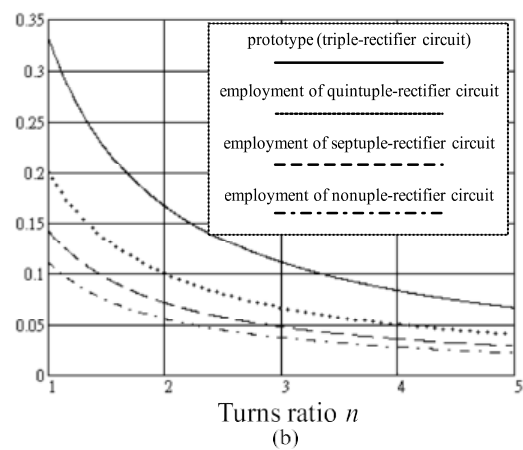
(b)

V. PERFORMANCE COMPARISONS

The performance comparison of the proposed isolated converter and other high step-up isolated converters introduced for demonstrating the performance of the proposed converter. The below table shows the performance comparisons between the proposed and other high step-up isolated converters.

The high step-up isolated converters introduced can simultaneously satisfy electric-isolation and safety regulations. Both converters use two switches, a coupled inductor, and a switched capacitor to achieve high step-up conversion.

PERFORMANCE COMPARISON TABLE

High Step-Up Isolated Converters	Converter in [25]	Converter in [26]	Proposed Converter
Voltage Gain	$n/\,1\text{-}D$	$n\,(2\text{-}D)/1\text{-}D$	$n\,(2\text{-}D)/(1\text{-}D)2$
Voltage Stress on Switch	$\dfrac{V_o}{n}$	$(1\text{-}D)Vo/\,n\,(2\text{-}D)$	$(1\text{-}D)Vo/\,n\,(2\text{-}D)$
Maximum Voltage Stress on Diode	V_o	$V_o/\,2\text{-}D$	$V_o/\,2\text{-}D$
PWM Control	Normal	Easy	Easy
Input Current Ripple	Large	Large	Normal

Converter in [25]	Active-clamp forward-flyback converter
Converter in [26]	Double-ended forward-flyback converter
Proposed Converter	Cascade double-ended boost-forward-flyback converter

The voltage gain of the proposed converter is the highest, and the voltage stresses on the power switches are the lowest. The PWM control of the proposed converter is simple,and the proposed converter possesses continuous and smooth input current, which decreases the conduction losses, lengthens lifetime of the input source, and constrains conducted EMI problems. In addition, the proposed converter achieves an extra cascade voltage gain for its boost converter by adding only one more inductor and one more capacitor than the comparison converter. Thus, the proposed isolated converter is suitable for high step-up applications with electric isolation.

VI. RESULTS AND DISCUSSION

The PV panel is used for the input source and the MOSFET is used as the electronic power switch of low voltage is used as it has low resistance and the switch undergoes low stress due to the coupled inductor and capacitor which recycles the leakage energy back to the circuit. The input voltage is kept at 40 v and the output voltage is achieved at 380 v which is a approximate 9 times voltage gain.
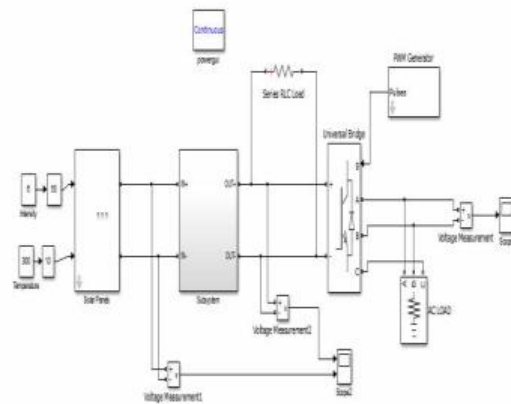
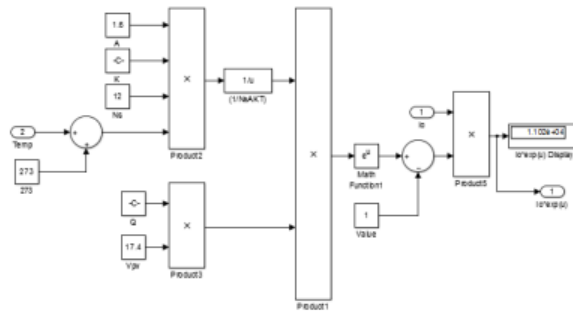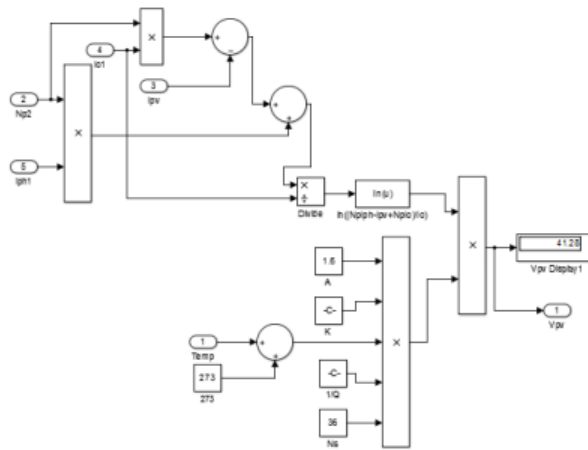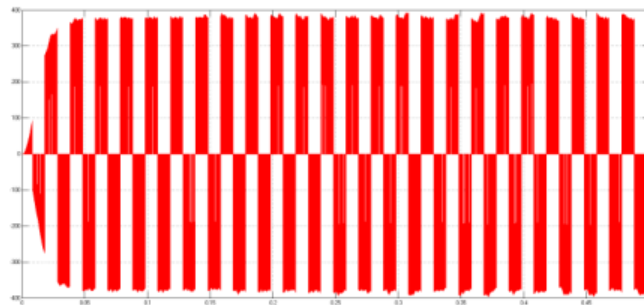# VII SIMULATION CIRCUIT OF THE PROJECT
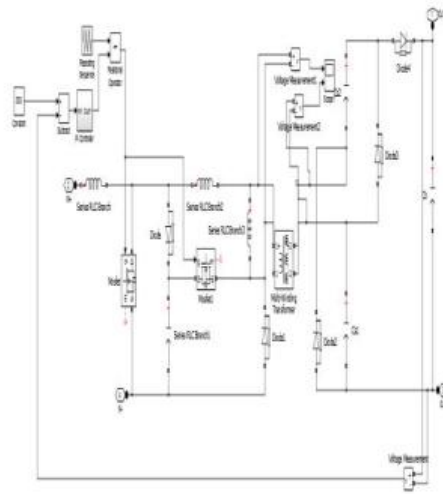
SIMULATION CIRCUIT

PI CONTROLLER

converter circuit

Solar panel subsystem

PV array with display
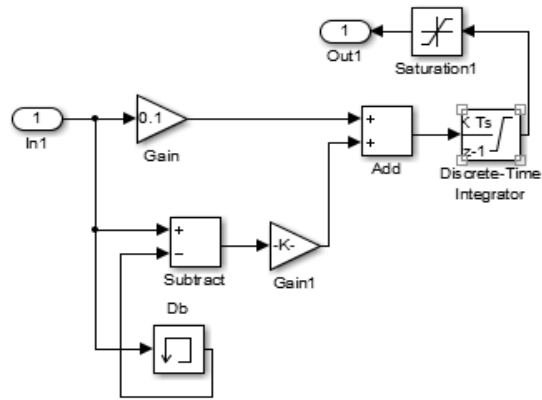
pv sub system

Sub system

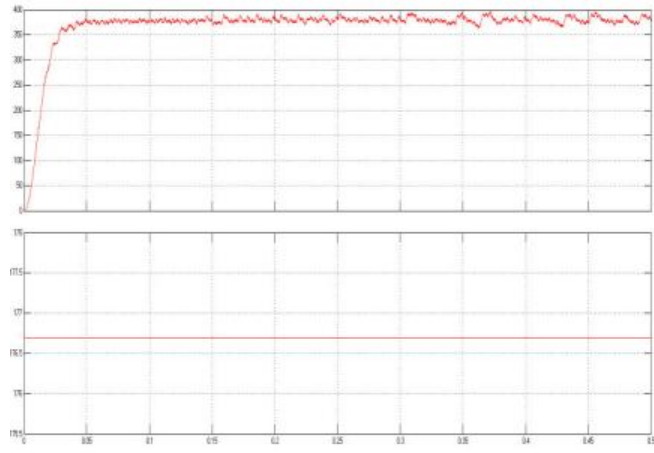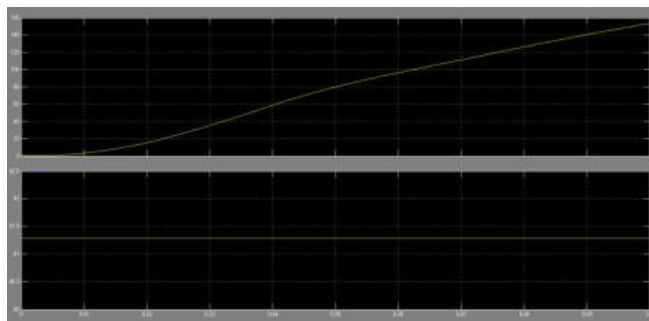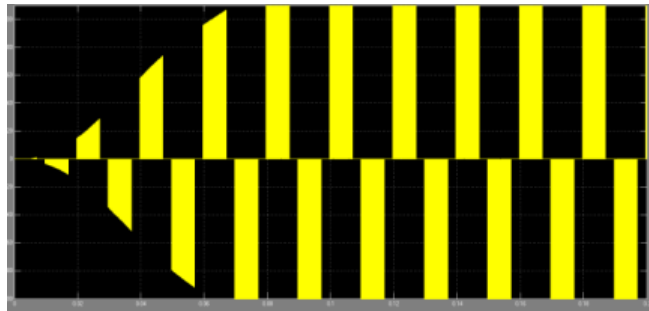**Pv Sub systems**

OUTPUT WAVEFORMS

VIII. CONCLUSION

This topology makes the input current continuous and smooth, which decreases the conduction losses and lengthens the lifetime of the input source and the constraints conducted EMI problems and lowers the voltage spikes across the power switches. In addition, the lossless passive clamp function recycles the leakage energy and lowers the voltage spikes across the power switches. Meanwhile, the voltage stress on the power switch is restricted and is much lower than the output voltage V_O, which is 380 V. Furthermore, the full-load efficiency is 90.67% at $P_o = 500$ W, and the maximum efficiency is 94.71% at $P_o = 200$ W. Thus, the proposed converter is suitable for renewable-energy applications that need high step-up conversion and have electrical-isolation requirements.

The scope of the second phase is the hardware implementation of the phase one.

IX REFERENCES

.
1. C. Zhang, S. Du, and Q. Chen, "A novel scheme suitable for high- voltage and large-capacity photovoltaic power stations," *IEEE Trans. Ind. Electron.*, vol. 60, no. 9, pp. 3775–3783, Sep. 2013.
2. B. N. Alajmi, K. H. Ahmed, S. J. Finney, and B. W. Williams, "A maximum power point

3. tracking technique for partially shaded photovoltaic systems in microgrids," *IEEE Trans. Ind. Electron.*, vol. 60, no. 4, pp. 1596–1606, Apr. 2013.
4. E. S. Sreeraj, K. Chatterjee, and S. Bandyopadhyay, "One-cycle- controlled single-stage single-phase voltage-sensorless grid-connected PV system," *IEEE Trans. Ind. Electron.*, vol. 60, no. 3, pp. 1216–1224, Mar. 2013.
5. S. V. G. Oliveira and I. Barbi, "A three-phase step-up DC–DC converter with a three-phase high-frequency transformer for DC renewable power source applications," *IEEE Trans. Ind. Electron.*, vol. 58, no. 8, pp. 3567–3580, Aug. 2011.
6. S. Dasgupta, S. N. Mohan, S. K. Sahoo, and S. K. Panda, "Lyapunov function-based current controller to control active and reactive power flow from a renewable energy source to a generalized three-phase micro- grid system," *IEEE Trans. Ind. Electron.*, vol. 60, no. 2, pp. 799–813, Feb. 2013.
7. S. Dasgupta, S. N. Mohan, S. K. Sahoo, and S. K. Panda, "Application of four-switch-based three-phase grid-connected inverter to con nect renewable energy source to a generalized unbalanced microgrid system," *IEEE Trans. Ind. Electron.*, vol. 60, no. 3, pp. 1204–1215, Mar. 2013.
8. W. Li and X. He, "Review of nonisolated high-step-up DC/DC converters in photovoltaic grid-connected applications," *IEEE Trans. Ind. Electron.*, vol. 58, no. 4, pp. 1239–1250, Apr. 2011.
9. W. Li, X. Xiang, C. Li, W. Li, and X. He, "Interleaved high step-up ZVT converter with built-in transformer voltage doubler cell for distributed PV generation system," *IEEE Trans. Power Electron.*, vol. 28, no. 1, pp. 300–313, Jan. 2013.
10. K.-C. Tseng, C.-C. Huang, and W.-Y. Shih, "A high step-up converter with a voltage multiplier module for a photovoltaic system," *IEEE Trans. Power Electron.*, vol. 28, no. 6, pp. 3047–3057, Jun. 2013.
11. S.-M. Chen, T.-J. Liang, L.-S. Yang, and J.-F. Chen, "A safety enhanced, high step-up DC–DC converter for AC photovoltaic module applica- tion," *IEEE Trans. Power Electron.*, vol. 27, no. 4, pp. 1809–1817, Apr. 2012.
12. C.-T. Pan and C.-M. Lai, "A high-efficiency high step-up converter with low switch voltage stress for fuel-cell system applications," *IEEE Trans. Ind. Electron.*, vol. 57, no. 6, pp. 1998–2006, Jun. 2010.
13. Y.-P. Hsieh, J.-F. Chen, T.-J. Liang, and L.-S. Yang, "Novel high step-up DC–DC converter with coupled-inductor and switched-capacitor techniques for a sustainable energy system," *IEEE Trans. Power Electron.*, vol. 26, no. 12, pp. 3481–3490, Dec. 2011.
14. S. Selvakumar, Dr.S.Ravi, "Adaptive Modulation IN Reconfigurable Platform" Journal of Theoretical and Applied Information Technology. Vol 68, PP 108-114, Oct 2014
15. C. Evangelista, P. Puleston, F. Valenciaga, and L. M. Fridman, "Lyapunov-designed super-twisting sliding mode control for wind energy conversion optimization," *IEEE Trans. Ind. Electron.*, vol. 60, no. 2, pp. 538–545, Feb. 2013.
16. R. Li and D. Xu, "Parallel operation of full power converters in permanent-magnet direct-drive wind power generation system," *IEEE Trans. Ind. Electron.*, vol. 60, no. 4, pp. 1619–1629, Apr.   2013.
17. S.-K. Changchien, T.-J. Liang, J.-F. Chen, and L.-S. Yang, "Novel high step-up DC–DC converter for fuel cell energy conversion sys- tem," *IEEE Trans. Ind. Electron.*, vol. 57, no. 6, pp. 2007–2017, Jun. 2010.
18. W. Li, L. Fan, Y. Zhao, X. He, D. Xu, and B. Wu, "High-step-up and high-efficiency fuel-cell power-generation system with active-clamp flyback–forward converter," *IEEE Trans. Ind. Electron.*, vol. 59, no. 1, pp. 599–610, Jan. 2012.